



ISSN: 2321-2152



IJMECE

*International Journal of modern
electronics and communication engineering*

E-Mail

editor.ijmece@gmail.com

editor@ijmece.com

www.ijmece.com

CUTTING PERFORMANCE AND SURFACE INTEGRITY IN SUPERALLOY INCONEL 718 END FACE MILLING: THE INFLUENCE OF VARIOUS COOLING AND LUBRICATION CONDITIONS

Mrs. K. Devadharshini, Mr. S. Samraj, Mr. K. Sedhuramalingam, Dr. L. Vigneash

Assistant Professor ^{1,2,3} Associate Professor ⁴

devadharshini.k@actechnology.in, ssamraj@actechnology.in,

sedhuramalingam.k@actechnology.in, dr.vigneashl@actechnology.in

Department of MCT, Arjun College of Technology, Thamaraiikulam, Coimbatore-Pollachi
Highway, Coimbatore, Tamilnadu-642 120

ABSTRACT:

Inconel 718 is a superalloy made of nickel that has exceptional mechanical and thermal properties. However, producing this material is difficult since it releases a great deal of heat. If you follow the correct cooling and lubrication (CL) procedures, it will cut much more effectively and keep the surface intact. Cryogenic minimum quantity lubrication cutting (CMQLC), cryogenic cutting (CC), dry cutting (DC), and flood cutting (FC) are the four strategies for cutting Inconel 718 that are compared in this article. Cutting forces, temperature, tool wear, chip size, Ra, microstructure, and RS are some of the parameters that are assessed. The findings demonstrate that the addition of CL enhances processing. By comparison, DC produces an average temperature that is 55.47 degrees cooler than CMQLC. The least successful of the four treatments was CMQLC, which reduced the tool chipping area by 25% and dropped the surface Ra by 32.05%. With respect to RS, there was a 10.2% rise in subsurface influence depth, a 7.9% increase in TRS, and a 3.9% increase in MCRS. It is also possible to get a better RS state by using machining settings with a high mechanical thermal ratio. The CMQLC shows little signs of environmental pollution, excellent

optimal cutting performance, and surface integrity of the workpiece.

Important concepts include cutting performance, surface integrity, cooling and lubrication, Inconel 718, and cryogenic minimum quantity lubrication (CMQL).

1. INTRODUCTION

Inconel 718 nickel-based superalloy is widely used in aerospace engine turbine disks and blades, nuclear reactors, and other fields because of its low thermal conductivity, corrosion resistance, and anti-fatigue performance. Nevertheless, the excellent properties also make Inconel 718 one of the most difficult-to-cut materials. The cutting of Inconel 718 exhibits the characteristics of high coolant consumption, short tool life, and poor surface integrity. Although significant progress has been carried out in tools and cooling and lubrication (CL) strategies, the machining of Inconel 718 is still considered to be a huge challenge. During the cutting, about 98% of the energy is converted into heat, resulting in a significant rise in temperature at the cutting area. The addition of coolant can effectively cool the cutting zone compared to blocking heat generation¹ and reduce friction.² The machined

Table 1. Chemical composition of Inconel 718 (in % of mass).

Ni	Fe	Cr	Nb	Mo	F	Ti	Al	Ta	Co	Si	Mn
51.48	18.29	18.11	5.54	2.70	1.74	1.11	0.53	0.33	0.15	0.05	0.05

1. surface typically experiences tensile residual stress (TRS). Parts' fatigue life may be extended by increasing their hardness and decreasing their surface roughness, as well as by decreasing the TRS and producing compressive residual stress (CRS).⁴ Research on Inconel 718 for surface integrity prediction has shown a robust relationship between RS, fatigue life, and roughness.⁵ Therefore, research into how CL circumstances affect Inconel 718 cutting performance and surface integrity is required.

Cutting coolant costs may be significantly reduced with the help of CMQL, a technology that delivers cryogenic gas and lubricating oil all at once.⁶ With its excellent cutting capability and surface roughness, the CMQL has recently found widespread usage in cutting Ti6Al4V,⁷ AISI 316L,⁸ and AISI 1045.⁹ Lubricants that have a high friction coefficient but a low viscosity may increase tool life by as much as 200%.¹¹ In addition, the CMQLC makes short work of chip removal by reducing both thickness and friction.¹² Since Inconel 718 cutting generates a lot of heat, it's not clear whether even the tiniest drops may reach the cutting zone. When grinding Inconel 718, CMQL produces higher surface integrity than traditional cutting.¹³ CMQL's advantage in turning Inconel 718 is confirmed by analysing microstructure, surface roughness, cutting forces, tool wear, and surface roughness.¹⁶ While it may not have the same lubricating effect as emulsion oil, it is better for the environment and can attain above 90% FC.¹⁷ Then, greater cutting performance with less tool wear and less adhesion wear of chips are both achieved by using high-pressure coolant.¹⁸ The tool life is increased by 57% when the coolant use a cryogenic medium. beyond what is achieved at room temperature with 20% MQL and FC combined. By doing away with antiquated

methods of cooling and lubricating, CMQLC achieves a state of ecological harmony.^{19,20}

Tool wear and RS have been the primary foci of CL cutting studies on Inconel 718. Surface^{3,21} and modelling have been the primary areas of study about the RS that results after cutting.^{22,23} Few studies have thoroughly evaluated Inconel 718's cutting ability and surface integrity, particularly with regard to the RS at subsurface.²⁵ Therefore, Inconel 718 milling under DC, FC, CC, and CMQLC conditions is the subject of this study. We analyse the chips and measure the cutting forces and temperature.

Surface roughness, microstructure, and relative surface roughness are the metrics used to determine the surface integrity.

2. Setting up the experiment Characteristics of the component

Inconel 718, which has undergone heat treatment (γ HV 452), is used as the experimental material. The following information is derived from the experimental materials' elemental and metallic analyses and tensile tests.²⁶ Table also shows the primary chemical components.

1. Figure 1(a) shows the microstructure of Inconel 718, which consists of the following phases: d, g#, g##, and NbC. Figure 1(b) shows the stress-strain curve of heat-treated Inconel 718. At 20°C, the yield strength in MPa is 1308.6.

Experimental procedure

The DX6080 is used to conduct the milling experiment. A boundary dimension of 18 mm × 30 mm defines the workpiece's end surface. In addition, the substrate is the VSM-4E(D4) from ZCC.CT, and the tool is shown in Figure 2(b). Cemented carbide with an AlTiN coating is the substance in question.

Figure 2(a)–(c) displays the experimental setup. A refrigeration module and an oil mist module, each with its own volume and continuous injection, make up the bulk of CMQL equipment (PMPM15- S, SUNAIR, Figure 2(a)). The system is supplied with high-pressure gas (4-8 bar) via the pipeline, and the vortex nozzle is used to expel the cryogenic air (23°C measurement value). The oil mist module uses pulse control to transform vegetable oil-based lubricant into a mist that can be sprayed via the nozzle at a rate of 0.05-0.2 L/h. Referring to Table 2, choose values in the middle that fall within the tool's suggested range of cutting parameters.

Cutting forces are reduced, chips are shorted and removed, friction and scratches are reduced, and cutting becomes easier with high-pressure cryogenic flow. The oil mist acts as a lubricant, whereas compressed gas is primarily responsible for cooling in this system.²⁷

FC is filled with cutting fluid in the cutting region; DC does not impose any CL precautions. Both Figure 2(a) and (d) show the milling model that is helped by CMQL. In order to examine the cutting performance and surface integrity, the blue region designated on the workpiece undergoes a lengthy and steady cutting.

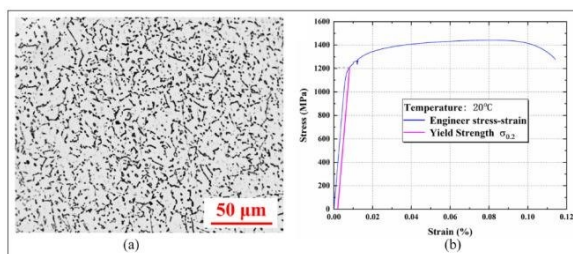


Figure 1. Microstructure and tensile properties of the Inconel 718 superalloy: (a) OM microstructure and (b) tensile stress-strain curve.

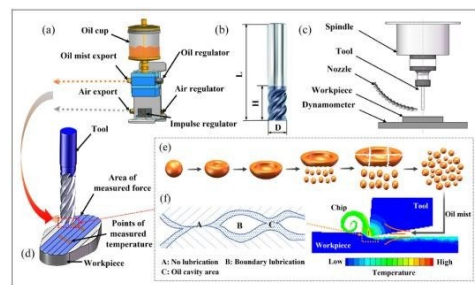


Figure 2. Experimental setup, milling, and lubrication models: (a) CMQL device (PMPM15-S), (b) tool model (VSM-4E), (c) the milling model, (d) experimental model, (e) breakage of oil droplets, and (f) lubrication model.

3. RESULTS AND DISCUSSION

Lubrication mechanism

We derive the CMQL lubrication model and the oil droplet breaking model from the theory of liquid sprays²⁸ and fluid dynamics, respectively. Figure 2(e) shows the oil droplet breaking. Lubricant atomisation boils down to the fact that droplets disintegrate and split when subjected to an external force. There is continual competition between surface tension, Table 2, and external forces (such as nozzle extrusion pressure) in this process. The criteria for cutting.

Cutting speed (r/min)	Feed rate (mm/min)	Axial depth (mm)	Radial depth (mm)
1800	500	0.20	0.50

viscosity of droplets. Because the surface tension allows making the droplets to maintain a simple spherical, the surface energy of the whole droplets is minimized; and

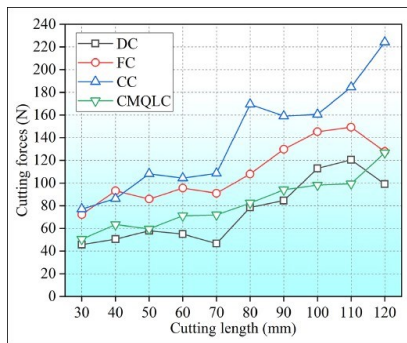


Figure 3. The variation of cutting force with the CL condition.

Oil droplets are unable to distort liquids due to their high viscosity. Separation of droplets occurs when the external force acting on them exceeds the sum of the liquid's surface tension and viscosity. Figure 2(f) shows the CMQL lubricating mechanism. This means that when the nozzle sprays droplets, the surface of the droplets will experience a vibration wave caused by the gas vibrations close to the jet path, which will progressively intensify. The droplets will first shatter into several smaller ones, before eventually forming lengthy droplets and flake liquid. Nozzle structure, jet state, and environmental factors all play a role in determining the size. The next step is to break the droplets apart and atomise them, which means that they will shrink in size by a variety of crushing processes brought about by the high-speed airflow. The ellipsoid, cumuliform, and semi-bubble shapes of the droplets are all affected by environmental factors including gas pressure. The semi-bubble droplets start to rupture at their apexes, forming annular liquid bands, when the jet's velocity exceeds the threshold. The annular liquid bands may hold 70% of the mass of the full oil droplets before injection since their volume is proportional to the size of the droplets before breaking. The high-speed jet further crushes the droplets, causing them to split into flakes on the surface and break into microbubbles in the inside. Eventually, all of the drops

A portion of the droplets are microdroplets, which are smaller than 2 millimetres.

The lubricating effect of oil is directly proportional to its volume, according to the hypothesis of the boundary lubrication film generated by coolant between two contact surfaces. Injecting a certain quantity of oil mist significantly affects the film's ability to keep moving. Figure 2(f) shows that oil cavity region (C), boundary lubrication (B), and no lubrication (A) in the cutting area.

Plus, the CMQL only processes a fraction of the oil mist that the coolant does. Further, the tool's elevated temperature and pressure prevent any droplets from reaching the contact region. Therefore, boundary lubrication is the most common kind of liquid friction at the interfaces of tools and workpieces, and total liquid friction between chips and workpieces is difficult to achieve. While cutting metal, large droplets transform into the paste, which then adheres to both the tool and the workpiece. Water evaporates more quickly from the contact zone and is better able to reach the cutting zone when droplets are smaller.⁹ So, improved surface wettability may be achieved by using small oil droplets, which lower the cutting force and friction coefficient.³⁰ The ability to dissipate heat is greatly enhanced by increasing the atomised air pressure, which in turn increases the wetting area. Hence, the residual stress reduction works.³¹ Oil droplets of a smaller size are therefore better for cutting.

Cutting forces

A Kistler dynamometer (9257B), An A/D data acquisition board, a charge amplifier, a data collector, and acquisition software (DynoWare) make up the cutting forces measuring system. Figure 3 shows the average cutting force as a function of cutting length. There is a dramatic rise in cutting forces at 80 mm. At high temperatures, the hardness decreases compared to lower temperatures, making cutting Although the DC forces are tiny, the fluctuation range is rather wide. Both the cutting forces and the stability of these forces are enhanced in FC.

The cutting forces are the most significant and unpredictable under CC because of the high levels of friction and tool wear. While both CMQLC and DC forces are quite tiny, the trend for CMQLC is more consistent. This is due to the fact that CMQLC offers superior lubrication, which helps to minimise friction in the cutting region. As a result, the cutting forces experienced by the CMQLC are minimal and consistent.

Cutting temperature

The cutting temperature is measured using a handheld infrared thermometer testo 868. Six measure points (Figure 2) are selected with stable cutting.

The temperature variation is shown in Figure 4(a) and the average is shown in Figure 4(b). The cutting temperature is affected by tool and CL, the temperatures obtained by four CL methods all show a trend of increase. DC and CC increase greatly, while FC and CMQLC increase slightly. DC has the largest amplitude because no CL is provided. Although the CC effectively cools the cutting area, it hardly reduces the heat from friction. Larger cutting forces lead to more intense vibration and severe tool wear. The CMQLC provides oil mist, which effectively reduces friction, and further reduces tool wear. The heat is taken away by the

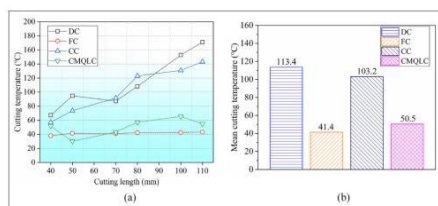


Figure 4. Cutting temperature variation with CL condition (a) and its average value (b).

coolant in a short time in FC. Whereas, due to the defects of the non-contact measurement itself, the actual cutting

temperature may be higher than theirs. And the FC still has the best cooling effect and provides water lubrication; the cutting temperature under CMQLC is also acceptable, so it is necessary to add lubricating medium in the cutting of high hardness materials such as Inconel 718.

Cutting edge chipping

The microscope (EASSON-EVM2515T) is used to examine the tool's wear. Critical parameters influencing surface integrity include tool wear and chipping, which increases heat and force, decreases the clearance angle, and increases the contact area between the tool and the workpiece. The shift in the subsurface is mostly driven by the enormous stress that they induce. Materials used in the work piece will undergo plastic deformation and expansion as a result of the high temperature.³² The tool's flank topography and end face are shown in Figure 5(a). In Figure 5(b), you can see the chipped area that corresponds. There is a lot of wear and tear on the tool's flank and cutting edge, and the chipping area reaches 0.19 mm² due to the high temperature and increased friction between contact pairs in DC. The coolant in FC lubricates the contact pairs, reducing friction and removing cutting heat and chips. The area that may be chipped decreases to 0.12 mm².

The cryogenic gas pre-cools the contact pairs, and the highest chipping is recorded in CC, reaching 0.26 mm². The tool's brittleness may rise somewhat, and the workpiece's surface hardens. Edge chipping happens due to the high immediate friction and impact force of the contact pairs in the absence of lubrication. Forces, temperature, and surface roughness all have a role in the succeeding cutting, which severely damages the tool and leads to worse surface quality. This is

consistent with the findings in Bagherzadeh et al.,7, demonstrating that cutting materials with high hardness, such Inconel 718, need lubrication in addition to cooling.

The CMQLC may be used to decrease the force and friction between the contact pairs. Area of chipping is 0.09 mm². The oil, however, will cling to a few surface flaws, leading to wear and tear. Finally, CMQLC causes the least amount of flank chipping, which means the tools last the longest.

Surface roughness

Surface morphologies acquired by cutting with the same parameters are detected using the InfinitFocus G4g 3D profile scanner from the ALICONA business. In order to get the surface cloud map and compute the Ra, a sample length of 4 mm was used. As shown in Figure 6, the surface is characterised. The amount of wear and tear on the surfaces of DC and CC varies with respect to their topographies. The surface is in bad condition in CC due to severe wear and scratches; the presence of an evident groove further confirms this. Perhaps due to the tool's severe damage, the Ra of CC is the greatest, reaching 3.397. Despite DC's lower Ra, the surface damage it experiences is more severe due to high temperature and large friction. Also, not all chips are fired at the correct moment. As a whole, FC has a level surface, without

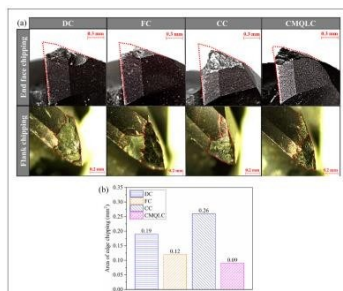


Figure 5. Tool chipping under different CL conditions: (a) topography of edge chipping and (b) areas of flank chipping.

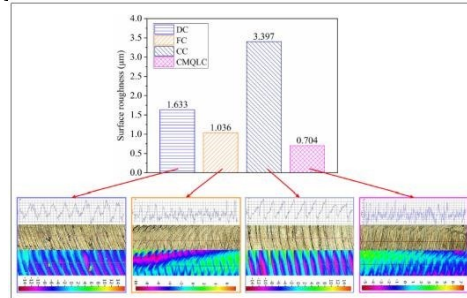


Figure 6. Surface roughness and morphology under different CL conditions.

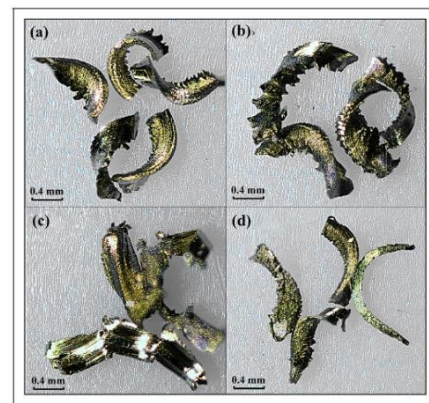


Figure 7. Chip morphology under different CL conditions:

(a) DC, (b) FC, (c) CC, and (d) CMQLC

scratches, and with less wear. Compared to DC (Ra 1.633) and FC (Ra 1.036), the CMQLC obtains relatively minimal surface roughness (Ra 0.704) due to its excellent CL effects. The surface profile generated by CMQLC may be messy because the tiny chips are adhered to the surface by oil, but CMQLC is still considered to be the best way.

Chip morphology

Under the microscope, you can see the shape of the chip as well. The cutting area temperature is determined by the heat that is produced and dissipated. Depending on the chip's heat dissipation capability and the development of material removal rate, mechanical load and thermal impact play a significant role in machining deformation.

has good benefits. Therefore, surface integrity is highly affected by chip shape.³³

The chip morphologies are shown in Figure 7. Serrated edges and more consistent chip quality are the results of DC processing. A serrated edge emerges when the shear plane becomes a shear body and the shear angle decreases due to rising pressure in the shear zone. Axial shear happens in the direction of the fractures that form on the free surface when the material approaches its strain limit. Serrated chips are formed when fractures and adiabatic shear work together. The chip takes on a spiral pattern when coolant is poured on; its curling degree is diminished; its length is somewhat amplified; and its serrated edge is expanded. This could be because the reduced temperature is insufficient to generate significant bending in the chip, resulting in a longer chip length when the

temperatures, the friction force under oil mist lubrication is small, and the squeezing effect is weakened. This type of chip facilitates material removal and reduces surface damage.

Microstructure

To analyse the subsurface metallographic structure, the sample surface is mechanically ground and polished, and the microstructure is studied with a metallographic microscope (Leica DM2700 M) and scanning electron microscope (ZEISS EVO 18). According to Pusavec et al.⁴, when the cutting strength is minimal, the fibre structure does not undergo any notable changes. Grain plastic deformation is mostly associated with tool wear and cutting force, whereas the mechanical effect is the most important factor in cryogenic cutting.³⁴ Cutting pressures are higher and granular plastic deformation is more noticeable as tool wear becomes more severe. One potential detrimental surface integrity feature is the processing-induced white layer (WL).³⁵ If you look at Figure 8, you can see the metallographic microstructure. There are a few surface fractures, some grain crushing on the subsurface, and WL (2 mm) occurs beneath the DC, suggesting that WL is more prone to develop at higher temperatures and with worn tools.

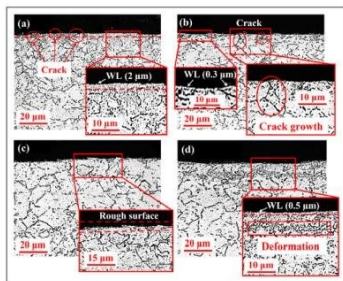


Figure 8. The metallographic structure under different CL conditions: (a) DC, (b) FC, (c) CC, and (d) CMQLC.

breaks. When using the cryogenic method, the chip no longer presents regular morphology but appears extrusion chip with fewer or no serrated edges. The chip brittleness increases at low temperatures, and it is easier to break. Nevertheless, the cutting edge of the tool with large wear is blunt, and the chips are mainly caused by extrusion and cracking. When the CMQLC method is adopted, the chip is narrow, the curling degree is small, and the edge sawtooth is not obvious. The chip-breaking performance is good at low

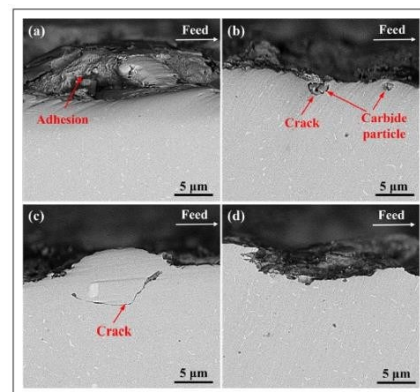


Figure 9. The metallographic structure under different CL conditions: (a) DC, (b) FC, (c) CC, and (d) CMQLC.

It seems as if the plastic deformation layer (PDL) is more akin to a microstructure layer that dynamically recovers. While FC reduced WL to around 0.3 mm, superficial fissures emerged and penetrated deeper into the material. Due to the tool's severe age, uneven cutting procedure, damaged surface's roughness and lower surface integrity, and lack of apparent cutting features in the microstructure, CC is the best course of action. The CMQLC analysis reveals a microstructure that is more akin to dynamic recrystallisation, with few surface fractures and a WL of around 0.5 mm. Subsurface grains exhibit clear plastic deformation, and the PDL depth is around 13 mm. This is due to the fact that cutting force and tool wear are the primary causes of grain plastic deformation, and the mechanical impact is therefore more prominent.³⁴ Using coolant may greatly decrease the WL depth, and CMQL can be used to determine the PDL, which improves fatigue life. The scanning electron micrographs of the processed cross-section of the object are shown in Figure 9. What we call the adhesion phenomenon happens in DC. This happens because cold welding takes place at high temperatures, increasing the material's affinity, which causes the material to stick to the workpiece's surface. Although FC lessens the adhesion problem, it causes fractures to form at hard particles. The lack of a lubricating liquid and the tool's chipping create a great mechanical stress under CC, which causes subsurface fractures to emerge and perhaps grow. There are benefits to using CMQL to lessen surface cracking and increase fatigue life, since both chipping and cracking are reduced.

Residual stress

The X-Ray Diffraction (Bruker, D8) technique is used to measure the RS, using the $\sin^2\psi$ method and the Mn target. These five benchmarks are

implemented over all strategies, and then

average them. Each electrolysis has a depth of 5 mm and uses a mixture of electrolyte, CH₃OH(90%), and HClO₄4%.

The major cause of RS is cutting with unequal plastic deformation. Structure yield strength is reduced by the CRS, which is often advantageous, and by the TRS, which is typically negative. When it comes to fatigue life, crack corrosion, fracture, and wear resistance, among other operating qualities, the RS is crucial.³⁶ Surfaces exhibit TRS as a result of the thermal effect and CRS as a result of the mechanical effect.³⁷ As shown in Figure 10(a), the RS varies with depth. This is

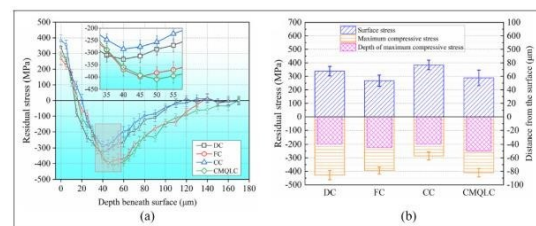


Figure 10. Residual stress under different CL conditions: (a) variation trend and (b) stress characterization.

found that TRS is always the surface stress, with lower values for FC and CMQLC; CRS is the predominant subsurface RS due to increased mechanical load and plastic deformation flow. At a depth of about 20 mm, the TRS quickly changes into CRS, and CRS quickly rises as depth increases. At 40, 45, 40, and 50 mm below surface, respectively, DC, FC, CC, and CMQLC achieve maximum compressive residual stress (MCRS). After CMQLC, FC, and CC, the CRS that DC reaches is the biggest of the bunch. Its anti-fatigue performance is best when Ra is small and CRS amplitude value is large. CMQL has a very high CRS amplitude value of 2409.43 MPa and the lowest Ra value of 0.704. Okay, then

$$\lambda = (R_{s_{max_compressive}} \cdot Depth - R_{s_{surface}}) \cdot 10^{-4} \quad (1)$$
 a method that offers superior resilience to fatigue. Furthermore, as a reference for characterising with excellent TRS, the surface TRS decreases with increasing MCRS and positioning depth (Figure 10(b)). To stand in for the aforementioned characterisation reference, we suggest using a weight parameter λ , which may be determined using formula (1). A, 1.68, 1.75, 1.10, and 2.02 are the four CL approaches. The RS extends the life of components to a greater extent when λ becomes bigger.

where MCRS is the maximum compressive stress ($R_{s_{max_compressive}}$), depth is the depth in millimetres, and $R_{s_{surface}}$ is the surface RS (MPa). Conversely, surface RS is affected by cutting force and temperature. ϵ The force-heat ratio ϵ is determined using Formula (2), with values of 0.662 for DC, 2.650 for FC, 1.339 for CC, and 1.617 for CMQLC.

According to the results, a high ϵ helps lower TRS, has a larger CRS, and is deeper. Despite having the greatest ϵ , FC is linked to higher coolant costs and environmental issues. In contrast, while working under cryogenic settings, when high temperatures might occur from severe tool wear, TRS can rise in tandem with the temperature, and CRS increases rapidly as depth increases, matching the findings of Bagherzadeh et al.7 A longer fatigue life of the workpiece is likely to be achieved by cutting under circumstances with a higher ϵ .22

$$\epsilon = \frac{\sum F_1 + F_2 + \dots + F_n}{nT} \quad (2)$$

Where F_1 – F_n is the average cutting force of n measuring areas, N ; t is the average cutting temperature, °C. By considering the effect of residual stress on fatigue life, the cost of coolant, and environmental

protection, CMQL is the optimized CL condition for cutting Inconel 718 superalloy.

4. CONCLUSION

In order to enhance the efficiency of machining and the longevity of Inconel 718 parts, this study compares and analyses the material's cutting performance and surface integrity in four CL modes: DC, FC, CC, and CMQLC. Here are the key findings: (1) Among the three methods, the CMQLC offers the most effective cutting performance in the long run. Cutting forces may be made smaller and more consistent with the help of CMQLC. When compared to DC, the average cutting temperature is 55.47 degrees lower. The compact, smooth surface allows for efficient discharging of the short, non-serrated chips. The tool has had a 25% reduction from FC, making it the area with the least amount of chipping.

In regards to the surface integrity gained by cutting Inconel 718, the CMQL has a clear advantage. The FC value is 32.05 percent higher than the lowest R_a that was achieved under the CMQL condition. There is a 0.5 mm thick white layer and a 13 mm deep PDL. In comparison to FC, CMQLC yields a 7.9% bigger TRS, and it also acquires a subsurface MCRS and an influence depth that are 3.9% and 10.2% larger, respectively, than FC. Increasing the force-heat ratio during cutting may enhance RS both underneath and on the surface, which in turn can lengthen the fatigue life.

Thirdly, the coolant's cooling function is enhanced since the FC dissipates a significant amount of heat. Thanks to CMQL's oil mist lubrication, the surface sticks better.

very small cracks, resulting in fine scuffs. Although it has the finest surface polish, it somewhat alters the overall surface roughness. The tool also experienced significant wear and chipping due to the fact that cryogenic gas pre-cools the cutting surface without applying any lubricant. Consequently, it is not appropriate to cool high-hardness materials without first applying lubricant.

(4) A research on cutting performance and surface integrity found that CMQL offers the highest complete performance while cutting Inconel 718. A better CRS dispersion, longer tool life, less coolant consumption, and a smoother surface are some of its advantages.

REFERENCES

- Mia M, Rahman MA, Gupta MK, et al. Advanced cooling-lubrication technologies in metal machining. In: Pramanik A (ed.) *Machining and tribology*. Amsterdam: Elsevier, 2022, pp.67–92.
- Anand N, Kumar AS and Paul S. Effect of cutting fluids applied in MQCL mode on machinability of Ti-6Al-4V. *J Manuf Process* 2019; 43: 154–163.
- Arunachalam RM, Mannan MA and Spowage AC. Residual stress and surface roughness when facing age hardened Inconel 718 with CBN and ceramic cutting tools. *Int J Mach Tools Manuf* 2004; 44: 879–887.
- Pusavec F, Hamdi H, Kopac J, et al. Surface integrity in cryogenic machining of nickel based alloy—Inconel 718. *J Mater Process Technol* 2011; 211: 773–783.
- Holmberg J, Wretland A, Hammersberg P, et al. Surface integrity investigations for prediction of fatigue properties after machining of alloy 718. *Int J Fatigue* 2021; 144: 106059.
- Sharma VS, Dogra M and Suri NM. Cooling techniques for improved productivity in turning. *Int J Mach Tools Manuf* 2009; 49: 435–453.
- Bagherzadeh A, Kuram E and Budak E. Experimental evaluation of eco-friendly hybrid cooling methods in slot milling of titanium alloy. *J Clean Prod* 2021; 289: 125817.
- Szczotkarz N, Mrugalski R, Maruda RW, et al. Cutting tool wear in turning 316L stainless steel in the conditions of minimized lubrication. *Tribol Int* 2021; 156: 106813.
- Maruda RW, Krolczyk GM, Feldshtein E, et al. Tool wear characterizations in finish turning of AISI 1045 carbon steel for MQCL conditions. *Wear* 2017; 372–373:54–67.
- Pereira O, Martí'n-Alfonso JE, Rodríguez A, et al. Sustainability analysis of lubricant oils for minimum quantity lubrication based on their tribo-rheological performance. *J Clean Prod* 2017; 164: 1419–1429.
- Chen J, Yu W, Zuo Z, et al. Tribological properties and tool wear in milling of in-situ TiB₂/7075 Al composite under various cryogenic MQL conditions. *Tribol Int* 2021; 160: 107021.
- Maruda RW, Krolczyk GM, Nieslony P, et al. Chip formation zone analysis during the turning of austenitic stainless steel 316L under MQCL cooling condition. *Procedia Eng* 2016; 149: 297–304.
- Naskar A, Singh BB, Choudhary A, et al. Effect of different grinding fluids applied in minimum quantity cooling-lubrication mode on surface integrity in cBN grinding of Inconel 718. *J Manuf Process* 2018; 36: 44–50.

14. Ostrowicki N, Kaim A, Gross D, et al. Effect of various cooling lubricant strategies on turning Inconel 718 with different cutting materials. *Procedia CIRP* 2021; 101: 350–353.
15. Gupta MK, Mia M, Pruncu CI, et al. Parametric optimization and process capability analysis for machining of nickel-based superalloy. *Int J Adv Manuf Technol* 2019; 102: 3995–4009.
16. Marques A, Paipa Suarez M, Falco Sales W, et al. Turning of Inconel 718 with whisker-reinforced ceramic tools applying vegetable-based cutting fluid mixed with solid lubricants by MQL. *J Mater Process Technol* 2019; 266: 530–543.
17. Pereira O, Catala` P, Rodri`guez A, et al. The use of hybrid CO₂ + MQL in machining operations. *Procedia Eng* 2015; 132: 492–499.
18. Polvorosa R, Sua´rez A, de Lacalle LNL, et al. Tool wear on nickel alloys with different coolant pressures: comparison of Alloy 718 and Waspaloy. *J Manuf Process* 2017; 26: 44–56.
19. Pereira O, Celaya A, Urbikai´n G, et al. CO₂ cryogenic milling of Inconel 718: cutting forces and tool wear. *J Mater Res Technol* 2020; 9: 8459–8468.
20. Pereira O, Urbikain G, Rodri`guez A, et al. Internal cryo-lubrication approach for Inconel 718 milling. *Procedia Manuf* 2017; 13: 89–93.
21. Boozarpoor M, Teimouri R and Yazdani K. Comprehensive study on effect of orthogonal turn-milling parameters on surface integrity of Inconel 718 considering production rate as constrain. *Int J Lightweight Mater Manuf* 2021; 4: 145–155.
22. Jiang X, Kong X, He S, et al. Modeling the superposition of residual stresses induced by cutting force and heat during the milling of thin-walled parts. *J Manuf Process* 2021; 68: 356–370.
23. Vovk A, So`lter J and Karpuschewski B. Finite element simulations of the material loads and residual stresses in milling utilizing the CEL method. *Procedia CIRP* 2020; 87: 539–544.
24. Jeyapandiarajan P and Anthony XM. Evaluating the machinability of Inconel 718 under different machining conditions. *Procedia Manuf* 2019; 30: 253–260.
25. De Bartolomeis A, Newman ST, Jawahir IS, et al. Future research directions in the machining of Inconel 718. *J Mater Process Technol* 2021; 297: 117260.